10.1109/ULTSYM.2012.0258

ULTRASOUND NDE IMAGING THROUGH REVERBERANT LAYERS VIA SUBSPACE ANALYSIS AND PROJECTION

Ramazan Demirli*, Moeness G. Amin, Yimin D. Zhang
Center for Advanced Communications, Villanova University, Villanova, PA 19085, USA

Abstract- In ultrasonic flaw imaging through reverberant layers, the top layer not only induces strong reverberation clutter but also repeats the flaw echo, giving rise to echo multiples. The reverberation clutter often overwhelms the target echoes, rendering the imaging of material flaws extremely difficult. Furthermore, echo multiples may obscure the identification of actual targets, especially when there are a number of targets in the scene. The reverberation clutter and flaw echo multiples must be suppressed or sufficiently mitigated in order to enable proper flaw imaging. In this paper, a subspace-based approach is utilized to suppress the reverberation clutter, followed by predictive filtering to suppress echo multiples. The clutter, due to its significantly high strength relative to the flaw echoes, is captured in the signal subspace that corresponds to the dominant eigenvalues of the data covariance matrix. It can be suppressed by applying orthogonal clutter subspace projection. Predictive deconvolution method is then used to suppress flaw echo multiples and enhance the visibility of the true flaw echoes in the presence of noise and clutter remnants. The effectiveness of the proposed imaging-through-layer approach is demonstrated via synthesized array data using real measurements of reverberation clutter and flaw echoes.

Index Terms - Ultrasound flaw imaging, reverberation removal, multiples suppression, subspace projection, predictive deconvolution.

I. INTRODUCTION

In ultrasonic imaging through layers, reverberations induced by the layer (i.e., the imaging screen) often mask the target echoes and make the detection and localization of material flaws or tissue abnormalities extremely difficult, if not impossible. Further, the layer also repeats the actual target echoes, giving rise to target multiples and thereby causing challenges in identifying the true targets and separating them from ghosts. Therefore, such reverberations (which are also referred to hereafter as reverberation clutter) and echo multiples must be suppressed or sufficiently mitigated in order to reveal the target echoes. The majority of existing approaches dealing with reverberation are based on the ideal acoustic wave propagation model in the layered media [1], [2], [3], [4], [5]. For example, Saniie and Nagle have developed analytical models of reverberation patterns measured from multi-layered media [1]. These models are used for the classification of echoes associated with each layer. The predictive deconvolution technique [6], commonly used in reverberation suppression in seismic explorations, has been applied to ultrasound reverberation suppression [2], [3]. This method also assumes, although implicitly, an ideal propagation model by relying on the repeatability of reverberating patterns.

Furthermore, the existing approaches often deal with ultrasonic measurements in the far field, as such, apply to immersion testing measurements. Consequently, they are not practical for field testing scenarios where only contact measurements can be performed in the near field of the transducer. Making contact measurements through the layer is further complicated by the coupling issues and strong irregular echoes from the layer's front surface. The reverberation patterns in these cases cannot be easily predicted and removed from the measurements.

This research is supported by National Science Foundation (NSF) under grant number IIP-0917690. (* Corresponding author: Dr. Ramazan Demirli, ramazan.demirli@villanova.edu)

Recently, we proposed an alternative approach based on reverberation subspace learning and projection for effective clutter suppression [7]. A similar approach has also been utilized in through-the-wall radar imaging to remove the wall clutter and enhance the visibility of indoor targets [8], [9]. In this approach, the clutter is removed by projecting the received signal onto a subspace that is orthogonal to the bases of clutter responses. The clutter subspace is constructed from the array data by exploiting the spatial coherency of the reverberation signals and incoherency of the flaw echoes.

In this paper we develop a method for the suppression of echo multiples, i.e., the repeats of flaw echoes due to multiple bounces within the top layer, to clearly reveal the flaw echoes. These multiples, even after reverberation suppression, appear as ghosts, causing cluttered image and uncertainty in the true target location. The problem becomes more challenging when there are multiple flaws in the scene. We address this problem by utilizing a predictive filtering approach for undoing channel convolution generating the echo multiples. Synthesized array data is used to demonstrate the effectiveness of the proposed through-the-layer imaging method.

The remainder of the paper is organized as follows. Section II reviews the clutter subspace construction and projection technique for array measurements. Section III presents a predictive deconvolution algorithm for multiples suppression. Section IV presents the results of imaging experiments with and without reverberation and multiples suppression. Section V concludes the paper.

II. CLUTTER REMOVAL USING SENSOR ARRAY DATA

A flaw imaging problem through a reverberant layer with a K-element sensor array is depicted in Fig. 1. The sensor array may consist of a number of physically present transducers or be formed from a single transducer through aperture synthesis. The signal received at the k-th sensor can be modeled as,

$$y_k(t) = \alpha_k s_f(t-\tau_k) + r(t) + n(t), \quad k = 0,1...K-1, \qquad (1)$$

where $\alpha_k s_f(t-\tau_k)$ denotes the flaw echo and its multiples received at the k-th sensor, $r(t)$ denotes the reverberation clutter due to the layer, and $n(t)$ denotes the additive white Gaussian noise (AWGN). The reverberation clutter is of quasi-periodic nature damped over time, where the periodicity and

978-1-4673-4562-0/12/$31.00 ©2012 IEEE

the degree of damping depend on the thickness and density of the layer. Under ideal measurement conditions (e.g., the layer is immersed in water in the far field), the reverberation signal can be well approximated as a superposition of time-shifted and amplitude-scaled replicas of the transducer pulse echo wavelet, $s_e(t)$, as

$$r(t) = \rho s_e(t) + \varsigma_{12}\varsigma_{21}\sum_{m=1}^{\infty}(-\rho)^{2m-1}s_e(t-2m\Delta T) \qquad (2)$$

where ΔT denotes the time-difference-of-arrival of successive echoes, ρ denotes the reflection coefficient from the propagation path to the layer, and $\varsigma_{12},\varsigma_{21}$ denote the transmission coefficients from the propagation path to the layer and layer to the propagation path, respectively. This analytical model can be interpreted as superimposed echoes with unknown delays and amplitudes [1]. The reverberation signal can be estimated using, e.g., a maximum likelihood estimation algorithm [10].

For contact measurements, the reverberation signal does not conform to the ideal model for a number of reasons. First, since contact measurements are performed in near field, the strong front-surface reflection at the transducer-layer interface makes the reverberating pattern much more complicated. Second, the reverberation signal varies from one measurement to another depending on the coupling between the transducer and the top layer as well as the bounding between the layer and the test material.

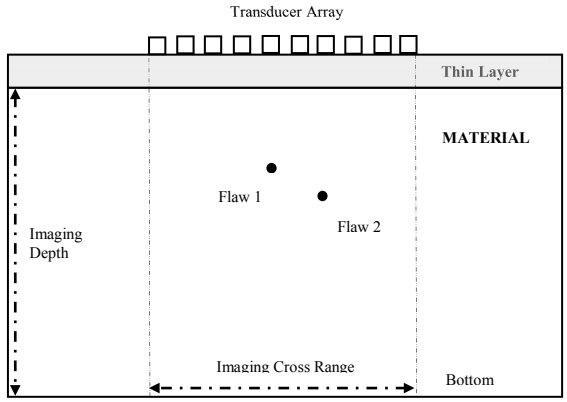

Figure 1. Experimental setup for flaw measurements through a layer.

We note that, while the reverberation clutter measurements vary in terms of local delays and small perturbations, the flaw echo (as well as its multiples) measurements vary from one sensor to another due to the distinct distance between a flaw and each sensor. The variation in the flaw echo is modeled in terms of the delays τ_k due to the spatial arrangement of the array sensors, and the weighting factors α_k due to the beam pattern of the transducers. Hence, the clutter reverberation measurements show high degree of spatial coherency, whereas the flaw measurements show incoherency. In order to exploit the coherency and the relative strength of reverberation clutter, we utilize a subspace construction and projection approach.

For clutter subspace construction, we concatenate the sensor array measurements into a data matrix of size $N\times K$ as

$$\mathbf{Y}_a = \left[\mathbf{y}_0 \quad \mathbf{y}_1 \quad . \quad . \quad \mathbf{y}_{K-1}\right] \qquad (3)$$

and then compute a covariance matrix estimate as,

$$\mathbf{C}_{\mathbf{Y}_a} = \frac{1}{K}\mathbf{Y}_a\mathbf{Y}_a^T = \mathbf{C}_r + \sigma_v^2\mathbf{I}, \qquad (4)$$

where $\mathbf{C}_r$ and $\sigma_v^2\mathbf{I}$ represent the clutter and noise covariance matrices, respectively, and $\mathbf{I}$ denotes the $N\times N$ identity matrix, $(.)^T$ denotes the transpose operation. $\mathbf{C}_{\mathbf{Y}_a}$ is decomposed into principal components using the eigenvalue decomposition,

$$\mathbf{C}_{\mathbf{Y}_a} = \sum_{m=1}^{M}\lambda_m\mathbf{u}_m\mathbf{u}_m^T \qquad (5)$$

where λ_m denotes the m-th eigenvalue in an non-increasingly ordered set $\lambda_1 \geq \lambda_2 \geq \ldots \geq \lambda_M$ and $\mathbf{u}_m$ denotes the corresponding eigenvector. M is determined by the number of array sensors and the spatial correlation of the received data signal, and is usually much smaller than N. The first η eigenvectors belong to the clutter subspace, whereas the remaining eigenvectors belong to the noise subspace. Since the dimension of the clutter subspace is not known *a priori*, it should be estimated. An information theoretic criterion, the Minimum Description Length (MDL) [7], is employed to estimate the clutter subspace dimension as,

$$\hat{\eta} = \arg\min_{\eta} N\ln\left(\frac{\left[\frac{1}{M-\eta}\sum_{m=\eta+1}^{M}\lambda_m\right]^{M-\eta}}{\prod_{m=\eta+1}^{M}\lambda_m}\right) + \frac{1}{2}\eta(2M-\eta)\ln N \qquad (6)$$

Then, the clutter subspace is formed by the first $\hat{\eta}$ dominant eigenvectors, i.e.,

$$\mathbf{U}_r = \left[\mathbf{u}_0 \quad \mathbf{u}_1 \quad . \quad . \quad \mathbf{u}_{\hat{\eta}}\right]. \qquad (7)$$

Finally, the clutter is removed from each sensor data by projecting onto the orthogonal subspace of the clutter to obtain flaw enhanced signals, i.e.,

$$\tilde{\mathbf{s}}_f^{[k]} = (\mathbf{I} - \mathbf{U}_r\mathbf{U}_r^T)\,\mathbf{y}_k. \qquad (8)$$

The above array data $\tilde{\mathbf{s}}_f^{[k]}$ contains the multiples of the target echoes which must be suppressed to properly reveal the target echoes. Towards this task, we present an adaptive predictive filtering approach in the next section.

III. MULTIPLES SUPPRESSION VIA PREDICTIVE DECONVOLUTION

An adaptive filtering approach for the suppression of flaw multiples is the predictive deconvolution (PD) technique [6]. If the layer properties (thickness and ultrasound velocity) are known, the period of multiples can be estimated. As such, the future samples of the repeating pattern of flaw multiples can be predicted based on the past samples. The prediction is performed through an FIR filter whose coefficients are optimized to minimize the prediction error. The coefficients

of an n-th order FIR prediction filter can be estimated by solving the following linear equations [6],

$$\begin{bmatrix} r_0 & r_1 & r_2 & \cdots & r_{n-1} \\ r_1 & r_0 & r_1 & \cdots & r_{n-2} \\ r_2 & r_1 & r_0 & \cdots & r_{n-3} \\ \vdots & \vdots & \vdots & \cdots & \vdots \\ r_{n-1} & r_{n-2} & r_{n-3} & \cdots & r_0 \end{bmatrix} \begin{bmatrix} a_0 \\ a_1 \\ a_2 \\ \vdots \\ a_{n-1} \end{bmatrix} = \begin{bmatrix} r_\alpha \\ r_{\alpha+1} \\ r_{\alpha+2} \\ \vdots \\ r_{\alpha+n-1} \end{bmatrix}, \quad (9)$$

where r_k denotes the auto-correlation of the clutter-suppressed signal (8) at correlation-lag k, $\{a_0, a_1, ..., a_{n-1}\}$ denote the prediction filter coefficients, and α denotes the prediction lag. The computational steps of the PD algorithm are outlined as:

1. Compute $(n+\alpha)$-lag autocorrelation of the input signal;
2. Compute prediction filter coefficients $\{a_0, a_1, ..., a_{n-1}\}$ via (9);
3. Convolve the input signal with prediction filter to obtain the *prediction signal*;
4. Delay the *prediction signal* by the *prediction-lag* α ;
5. Subtract the *delayed prediction signal* from the input signal.

We demonstrate the PD based multiples suppression on two simulated flaw echoes and their multiples as shown in Fig. 2. Fig. 2a depicts the two primary flaw echoes (marked as Flaw Echo 1 and Flaw Echo 2) and their multiples as if they were measured through a layer. Fig. 2b shows the echoes after their multiples are suppressed. The primary echoes are retained while their multiples are suppressed drastically. For this example, the filter length n and filter-lag α are set to 15% and 97% of the multiples' period, respectively. The robustness and performance of the prediction filter depends on these two parameters. We observed that using 10-20% and 95-100% of the period respectively for n and α perform quite well.

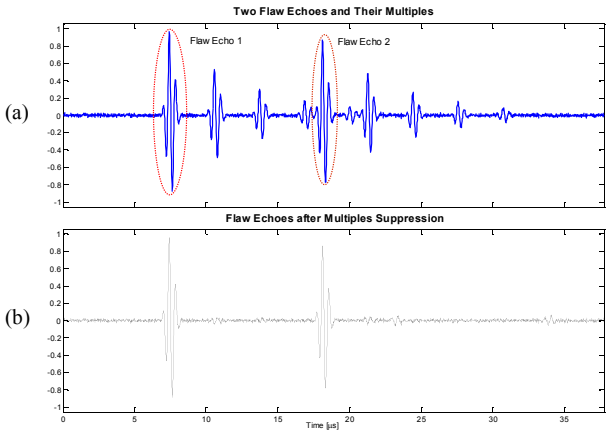

Figure 2. Multiples suppression via predictive deconvolution: a) Two simulated flaw echoes and their multiples as measured through a reverberant layer, b) The two flaw echoes after multiples suppression.

IV. Simulations and Experimental Results

4.1. Experiment Settings

An aluminum block (alloy number 6061) of dimensions 152 x 152 x 76 mm is used as a test specimen. A thin metal layer with 2 mm uniform thickness is coupled to the material with gel. The thin layer is highly reverberant and presents a challenging flaw imaging scenario. Fig. 1 shows schematic illustration of the test specimen, thin layer, and the synthesized transducer array used for ultrasonic measurements.

Transducer excitation and measurements are performed using an Olympus Panametrics Pulser/Receiver (P/R) (model 5072PR) operated in the monostatic (T/R) mode. The P/R settings are as follows: pulse repetition frequency (PRF) 1 KHz, energy level 3, damping level 4, amplifier gain 30 dB, low-pass filter with a cutoff frequency of 1 MHz, and high-pass filter with a cutoff frequency of 10 MHz. All the ultrasonic measurements are made with an Olympus single-element transducer (model V-110M) which has a center frequency of 5 MHz. The transducer is placed on the material surface with ultrasound coupling gel. The acquired signals are digitized with a digital scope (Agilent Technologies DSO7014A) at a sampling rate of 50 MHz. These signals are collected for 32 times and averaged internally by the scope to obtain a signal with an improved signal-to-noise ratio (SNR).

4.2 Simulations

We simulate an array measurement by moving a single-element transducer in small steps on the surface of the thin layer coupled to the material. To obtain flaw echoes impinged on reverberation, the flaw echoes are simulated based on the assumed flaw location, the geometry of the synthesized linear array, the respective delay between the flaw and sensors, and the beam pattern of the measuring transducer. The beam pattern is incorporated as a weighting factor on echo amplitudes based on the flaw location with respect to the transducer [11]. Furthermore, the flaw echo multiples are simulated based on the assumed thickness and velocity of the layer. To simulate an array data measured through a reverberant layer, we added these simulated flaw echoes to the 10 independent reverberation measurements obtained from the layer placed on the healthy sections of the aluminum block.

The subspace based clutter removal algorithm is evaluated on the synthetic array data containing 10 reverberation measurements superimposed with flaw echoes. Fig. 3a shows the two simulated flaw echoes and their multiples synthesized according to the assumed flaw locations as measured from the 4th element in the linear array (see Fig. 1). Fig. 3b shows the flaw echoes and their multiples added to the reverberation clutter to simulate the measured data through the layer at the 4th transducer. The above orthogonal subspace projection is applied to the signal in Fig. 3b. The reverberation-suppressed signal is shown in Fig. 3c. The flaw echoes and their multiples are mostly captured, although the remnants of reverberation clutter are still visible but weaker than the flaw echoes (compare Figs. 3a and 3c). Furthermore, the PD algorithm is applied to the signal in Fig. 3c. The primary flaw echoes become more dominant as shown in Fig. 3d. However, it is observed that the performance of multiples suppression is adversely affected by the remnants of reverberation clutter.

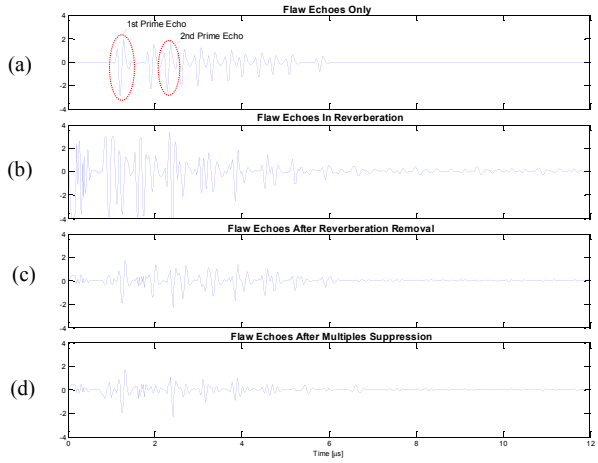

Figure 3. Reverberations and multiples suppression for imaging two flaws shown in Fig. 1: a) Simulated flaw echoes and their multiples as received by the 4th transducer, b) The flaw echoes and their multiples added to a real reverberation measurement, c) Flaw echoes after reverberation removal, d) Flaw echoes after multiples suppression.

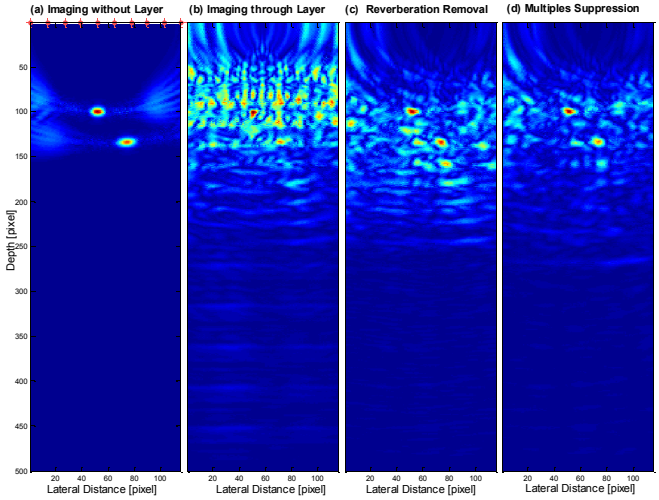

Figure 4. The synthetic aperture array imaging of two flaws through a layer as shown in Fig. 1: a) Imaging of flaws without the layer (1 pixel is 0.1mm), b) Imaging of flaws with the layer in heavy reverberation clutter, c) Imaging after reverberation suppression. The flaw and their multiples are dominant. d) Imaging after multiples suppression. The two flaws are clearly visible.

Finally, we demonstrate the flaw imaging capability of the subspace projection and multiples suppression techniques in the presence of heavy clutter. For this purpose, we utilized a receiver mode backprojection beamforming algorithm [12], [13], [14] adopted for synthetic aperture arrays as described in [7]. The imaging results are shown in Fig. 4. Fig. 4a shows the beamformed image of the two flaws in the test material without the thin layer. The positions of the array elements with respect to the flaw are shown on the top of the image in Fig. 4a. Fig. 4b shows the beamformed image when the flaws are measured through the layer. The flaws are invisible under strong reverberation clutter. Fig. 4c shows the beamformed image after clutter suppression using the proposed subspace projection. The reverberation clutter is suppressed drastically and the two flaw echoes become visible. However, the multiples of the flaw echoes still obscure the real targets. Fig. 4d shows the image after multiples suppression via PD. It is evident from Fig. 4 that the proposed algorithms enable proper visualization of flaw echoes which are otherwise overwhelmed by reverberation clutter and echo multiples.

V. CONCLUSIONS

In this paper, we dealt with ultrasound imaging of flaws in metallic objects through reverberant layers and addressed two major obstacles, i.e., the reverberation clutter and echo multiples. A subspace projection method was developed to suppress reverberation clutter, followed by predictive deconvolution algorithm to suppress echo multiples. The effectiveness of the proposed techniques was verified by imaging experiments involving a number of flaws in the scene. Furthermore, the proposed techniques can be incorporated into the existing array imaging systems with low complexity.

REFERENCES

[1] J. Saniie and D. Nagle, "Pattern recognition in the ultrasonic imaging of reverberant multilayered structures," *IEEE Trans. Ultrasonics, Ferroelectrics and Freq. Control,* vol. 36, no. 1, pp. 80-92, January 1989.

[2] D. Kishoni, "Removal of dominant reverberations from ultrasonic time-records of layered material by digital predictive deconvolution," in *Proceedings of Ultrasonics Symposium,* pp. 1075-1078, 1986.

[3] Y.-F. Chang, Y. Ma, C.-M. Lin, and J.-H. Lee, "Reverberation reduction in ultrasonic images via predictive deconvolution," *NDT&E International,* vol. 41, no. 1, pp. 245-241, January 2008.

[4] M. Duarte, J. Machado, and W. Pereira, "A method to identify acoustic reverberation in multilayered homogeneous media," *Ultrasonics,* vol. 41, pp. 683-698, 2004.

[5] K. Win, J. Wang, C. Zhang, and R. Yang, "Identification and removal of reverberation in ultrasound imaging," in *Proceedings of IEEE Conference on Industrial Electronics and Applications,* pp. 1675-1680, June 2010.

[6] O. Yilmaz, *Seismic Data Analysis: Processing, Inversion, and Interpretation of Seismic Data*, Tulsa: Society of Exploration Geophysics, 2000.

[7] R. Demirli, M. Amin, X. Shen, and Y. Zhang, "Ultrasonic flaw detection and imaging through reverberant layers via subspace analysis and projection," *Advances in Acoustics and Vibration,* vol. 2012, no. 957379, pp. 1-10, 2012.

[8] C. Debes, C. Weiss, A. M. Zoubir, and M. G. Amin, "Wall clutter mitigation using cross-beamforming in through-the-wall radar imaging," in *Proceedings of European Signal Processing Conference,* pp. 1097-1100, Aolborg, Denmark, August 2010.

[9] F. H. C. Tivive, A. Bouzerdoum, and M. G. Amin, "An SVD-based approach for mitigating wall reflections in through-the-wall radar imaging," in *Proceedings of IEEE Radar Conference*, Kansas City, KS, May 2011.

[10] R. Demirli and J. Saniie, "Model-based estimation of ultrasonic echoes. part II: Nondestructive evaluation applications," *IEEE Trans. Ultrasonics, Ferroelectrics, and Freq. Control,* vol. 48, no. 3, pp. 803-811, May 2001.

[11] R. Demirli, X. Rivenq, Y. D. Zhang, and M. G. Amin, "MIMO imaging for ultrasonic nondestructive testing," in *Proceedings of SPIE Conf. on Nondestructive Characterization Composite Materials, Aerospace Engineering, Civil Infrastructure*, San Diego, CA, March 2011.

[12] Y. Yoon and M. G. Amin, "High-resolution through-the-wall radar imaging using beamspace MUSIC," *IEEE Trans. Antennas and Propagation,* vol. 56, pp. 1763-1774, 2008.

[13] M. Amin, Ed., *Through-the-Wall Radar Imaging*, CRC Press, 2010.

[14] M. Amin and K Sarabandi, Special issue on remote sensing of building interior, *IEEE Transactions on Geoscience and Remote Sensing*, vol. 47, no 5, May 2009.